Atmospheric and
Environmental Research, Inc.

Algorithm Theoretical Basis Document (ATBD)
for the
Conical-Scanning Microwave Imager/Sounder (CMIS)
Environmental Data Records (EDRs)

Volume 7: Cloud EDRs
Part 2: Cloud Liquid Water EDR

Version 1.2 – 15 March 2001

Solicitation No. F04701-01-R-0500

Submitted by:
Atmospheric and Environmental Research, Inc.
131 Hartwell Avenue
Lexington, MA 02421-3126

With contributions by:
Alan Lipton, Sid-Ahmed Boukabara, Jennifer Hegarty,
Jean-Luc Moncet, Grant Petty Editor: Hélène Rieu-Isaacs

Prepared for:
Boeing Satellite Systems
919 Imperial Avenue
El Segundo, CA 90245

AER Document P757-TR-I-ATBD-CLW-20010315

This page intentionally left blank.

REVISION HISTORY

Version	Release Date	POC	Comments
1.0	1/16/01	A. E. Lipton, AER, Inc.	First Draft Version
1.1	1/20/01	A. E. Lipton, AER, Inc	Minor additions to background, algorithm description, and performance
1.2	4/2/01	A. E. Lipton, AER, Inc	Revised algorithm description and performance for precipitating clouds

RELATED CMIS DOCUMENTATION

Government Documents

Title	Version	Authorship	Date
CMIS SRD for NPOESS Spacecraft and Sensors	3.0	Associate Directorate for Acquisition NPOESS IPO	2 March 2001

Boeing Satellite Systems Documents

Title		Covering
ATBD for the CMIS TDR/SDR Algorithms		
ATBD for the CMIS EDRs	Volume 1: Overview	Part 1: Integration
		Part 2: Spatial Data Processing • Footprint Matching and Interpolation • Gridding • Imagery EDR
	Volume 2: Core Physical Inversion Module	
	Volume 3: Water Vapor EDRs	Atmospheric Vertical Moisture Profile EDR Precipitable Water EDR
	Volume 4: Atmospheric Vertical Temperature Profile EDR	
	Volume 5: Precipitation Type and Rate EDR	
	Volume 6: Pressure Profile EDR	
	Volume 7: Cloud EDRs	Part 1: Cloud Ice Water Path EDR
		Part 2: Cloud Liquid Water EDR
		Part 3: Cloud Base Height EDR
	Volume 8: Total Water Content EDR	
	Volume 9: Soil Moisture EDR	
	Volume 10: Snow Cover/Depth EDR	
	Volume 11: Vegetation/Surface Type EDR	
	Volume 12: Ice EDRs	Sea Ice Age and Sea Ice Edge Motion EDR Fresh Water Ice EDR
	Volume 13: Surface Temperature EDRs	Land Surface Temperature EDR Ice Surface Temperature EDR

Title		Covering
	Volume 14: Ocean EDR Algorithm Suite	Sea Surface Temperature EDR Sea Surface Wind Speed/Direction EDR Surface Wind Stress EDR
	Volume 15: Test and Validation	All EDRs

Bold = this document

TABLE OF CONTENTS FOR VOLUME 7, PART 2

LIST OF TABLES

LIST OF FIGURES

1 Introduction

1.1 Purpose

This algorithm theoretical basis document (ATBD) provides the underlying mathematical and theoretical background for Cloud Liquid Water (CLW) EDR (Environmental Data Record) for the Conical-scanning Microwave Imager/Sounder (CMIS) developed by Atmospheric and Environmental Research, Inc. (AER) in support of the National Polar-orbiting Operational Environmental Satellite System (NPOESS).

Retrievals of cloud liquid water (CLW) from microwave data are valuable for several applications. CLW has a strong impact on the optical properties of the atmosphere in the visible and infrared. This characteristic makes CLW a concern for operators of electro-optical sensors that view through the atmosphere and for climate studies concerned with radiative energy transfer. Phase changes between liquid and vapor or ice involve latent heat, which plays a significant role in development of weather systems and global energy transport.

1.2 Scope

The Core Physical Inversion Module of the CMIS EDR algorithms performs a major portion of the retrieval processing for the CLW EDR. That module is described in ATBD Vol. 2, which includes discussion of some aspects of the physics of the retrieval problem. The CLW algorithm under precipitating conditions is closely linked to the Precipitation EDR algorithm, which is described in ATBD Vol. 5. This document discusses physical aspects specific to CLW retrieval, presents the portions of the algorithm not covered by the Core Module or Precipitation volumes, and presents performance for the CLW EDR product.

2 Overview and Background Information

2.1 Objectives of the CLW EDR retrieval

The CLW EDR algorithm has the objective of deriving CLW reports from CMIS sensor data on a global basis in all weather conditions.

2.2 Summary of EDR requirements

2.2.1 Requirements from System Requirement Document

The text below and Table 2-1 are the portions CMIS System Requirements Document (SRD) section 3.2.1.1.1.1 that apply directly to the CLW algorithm.

Cloud liquid water is defined as the equivalent amount of water within cloud particles in a specified segment of a vertical column of the atmosphere. For this EDR, vertical cell size is the vertical height of the column segment and the vertical reporting interval specifies the locations of the column segment bottoms for which cloud liquid water must be reported.

Table 2-1: Cloud Liquid Water Requirement Table.

Para. No.	Parameter	Thresholds	Objectives
C40.4.5-1	a. Horizontal Cell Size	20 km	5 km
C40.4.5-2	b. Horizontal Reporting Interval	20 km	5 km
C40.4.5-3	c. Vertical Cell Size	N/A (Total Column)	0.3 km
C40.4.5-4	d. Vertical Reporting Interval	N/A (Total Column)	0.3 km
C40.4.5-5	e. Horizontal Coverage	Global	Global
C40.4.5-6	f. Vertical Coverage	N/A (Total Column)	0 - 30 km
C40.4.5-7	g. Measurement Range	0 - 5 kg/m^2	(TBD)
	h. Measurement Uncertainty		
C40.4.5-8	1. Over ocean	0.25 kg/m^2	0.01 kg/m^2
C40.4.5-9	2. Over land	0.5 kg/m^2	0.01 kg/m^2
C40.4.5-10	i. Mapping Uncertainty	7 km	1 km
C40.4.5-11	j. Swath Width	1700 km (TBR)	3000 km (TBR)

2.2.2 Interpretation of SRD Requirements

The definition of cloud water in the SRD suggests that precipitating particles are excluded. However, the measurement range stated in the requirement clearly extends to precipitating clouds. Therefore, we interpret the CLW requirement as covering both precipitating and non-precipitating clouds. Passive microwave measurements are unable to distinguish between suspended cloud liquid and falling liquid rain, as is illustrated later in this document. For

precipitating conditions, we therefore make the interpretation that the EDR is the total liquid water path, which includes both suspended and falling liquid water

2.3 Physics of Problem

Cloud liquid water may absorb and scatter microwave radiation. For non-precipitating clouds, the cloud particles are typically much smaller than the microwave wavelength. In this case, scattering in negligible and the Rayleigh absorption approximation applies, wherein absorption depends on liquid water path and is independent of the drop size distribution (Bohren and Huffman, 1983). In precipitating clouds, the liquid particles are large enough for scattering to be substantial (Gasiewski, 1992).

One mechanism by which cloud liquid can be detected with microwave measurements is the attenuation of radiation that has impinged on the cloud layer from below. This mechanism occurs whether the attenuation is caused by absorption or scattering. In the case of absorption, the cloud has an impact on the upwelling radiation if the effective radiating temperature of the cloud is different from that of the medium below. In the case of scattering, cloud liquid tends to decrease the top-of-atmosphere upward radiation because relatively warm-source radiation from the surface/lower troposphere is replaced by cooler-source radiation from the upper troposphere or space.

For ocean surfaces, the effective radiating temperature of upwelling radiation below cloud base is relatively low because the ocean has a relatively low emissivity and it strongly reflects radiatively cold cosmic radiation. Radiation emitted from cloud water has a warmer equivalent temperature than the background and provides a strong cloud signal. For land surfaces, the cloud emissive signal tends to be weak because the surface emissivities are commonly high enough that there is little difference between the effective emitting temperature of the surface and the temperature of the cloud.

The phenomenon of thermal contrast can provide some information regarding the altitude of cloud water. When the atmospheric temperature decreases with altitude, as it usually does in the troposphere, the emitting temperature of clouds decreases with increasing cloud altitude. This effect is mitigated, however, by the fact that the absorptance/emittance of the cloud decreases

with temperature (Lipton, et al., 1999). A higher cloud, therefore, has a lower temperature of emission but transmits more radiation from the warmer layers below.

Cloud liquid has a strong microwave signal over surfaces whose emission/reflection depends strongly on polarization, for microwave channels in "window" regions where the atmosphere is significantly transmissive. In such cases, the upwelling radiation at cloud base is substantially different in channels at the same frequency but different polarization. If there is little cloud liquid, the radiation that reaches the satellite is strongly polarized. As the cloud liquid increases, the degree of polarization decreases because the polarized radiation is absorbed and the cloud-emitted radiation is not polarized. Ocean surfaces have large emissivity differences between vertical and horizontal polarization, and are thus well suited for exploiting this phenomenon. For land surfaces, the polarization differences are much smaller and the cloud signal provided by this phenomenon is much weaker (Greenwald, et al., 1997).

In any precipitating cloud, there are particles with a wide range of sizes. The distribution of cloud water among the sizes varies substantially among clouds, even between clouds with the same precipitation rate. The "cloud" droplets are the particles that are too small to have significant fall speeds. From the perspective of radiative transfer, both the suspended and precipitating particles contribute to the absorption and emission of radiation, and the relative effects of each depend on the variable size distributions. The radiative effects of the non-precipitating particles are not sufficiently different from the effects of the precipitating particles to allow the two particle classes to be distinguished from passive microwave data. If an algorithm addresses only a specific class of precipitating clouds, there may be some skill at separating the cloud water from the precipitation on the basis of statistical relationships. Such statistical separation is not possible, however, for an algorithm that must function globally. Figure 2-1 illustrates that, even for modest rain rates, there is effectively no skill at retrieving cloud (suspended) liquid separately from the precipitating liquid when precipitation is present. The algorithm used to generate the results is statistical, so any correlations between precipitating and non-precipitating liquid are clearly not strong enough to be useful when a broad range of clouds is considered.

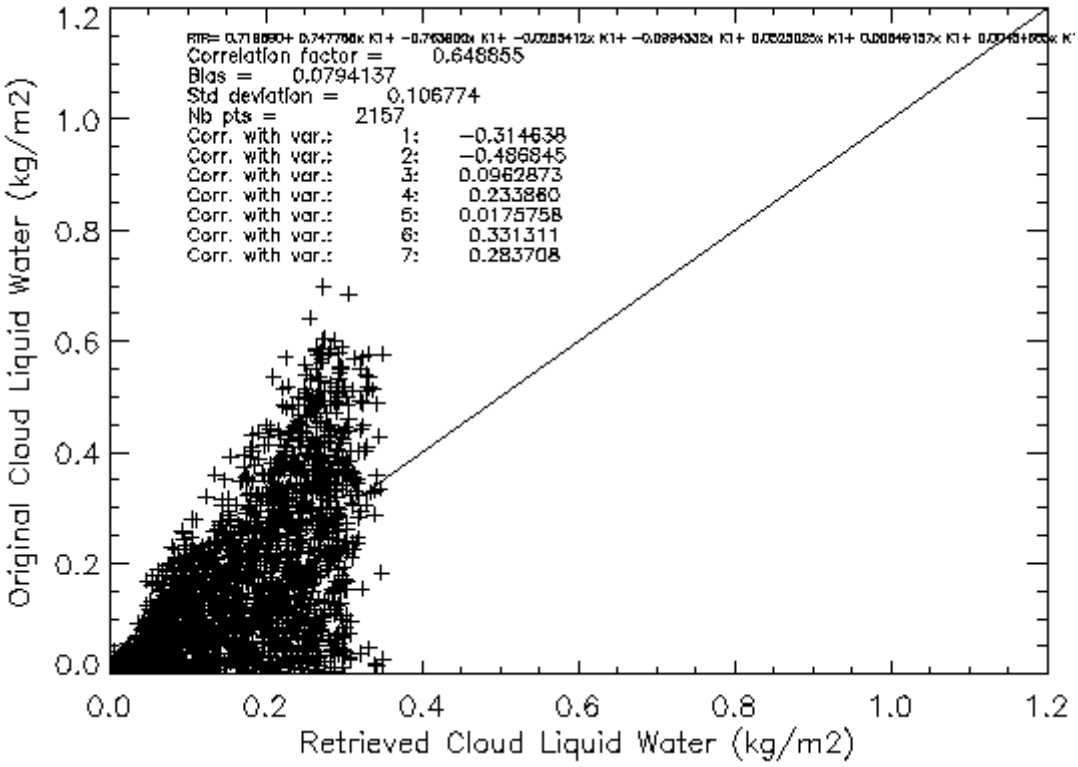

Figure 2-1: Results of simulated retrievals of suspended cloud liquid water within precipitating clouds. The test scenes were derived from the empirical cloud model of Kummerow. The algorithm was regression. A range of rain rates up to 10 mm/h were included.

2.4 Instrument Characteristics

The primary channels for cloud liquid water retrievals are the vertical and horizontally polarized window channels at 10, 18, 36, and 89 GHz. Among these channels, the higher frequencies provide more skill when the CLW is low and the lower frequencies provide more skill when the CLW is high, due to the trade-off between sensitivity and saturated response (Weng and Grody, 1994). The channels on the water vapor line at 23 GHz are essential also, for discriminating water vapor from liquid water. Additional information regarding water vapor and other environmental variables is provided by the channels at 166 and 183 GHz. The 50-GHz channels provide temperature profile information that assists in identifying thermal signals of clouds at the other frequencies.

We evaluated the potential for channels near the 118-GHz oxygen absorption line for profiling cloud water, in conjunction with the 50-GHz oxygen-band channels to account for the temperature profile component of the 118-GHz signal. We found, however, that the 118-GHz channels did not provide significant profiling skill in retrieval tests. The sensitivity of the brightness temperature in each channel to a perturbation of cloud liquid, when given as a function of the altitude of the cloud, is a very smooth, broad curve (Figure 2-2). Furthermore, the curves for each of a set of channels near the 118-GHz line have very similar shape, which means that the difference in brightness temperature between any two of the channels is insensitive to the cloud altitude. The 118-GHz channels are far short of the ideal, in which each channel has a strong sensitivity to cloud in a certain layer and minimal sensitivity elsewhere, with the respective channels having their peak sensitivities in different layers.

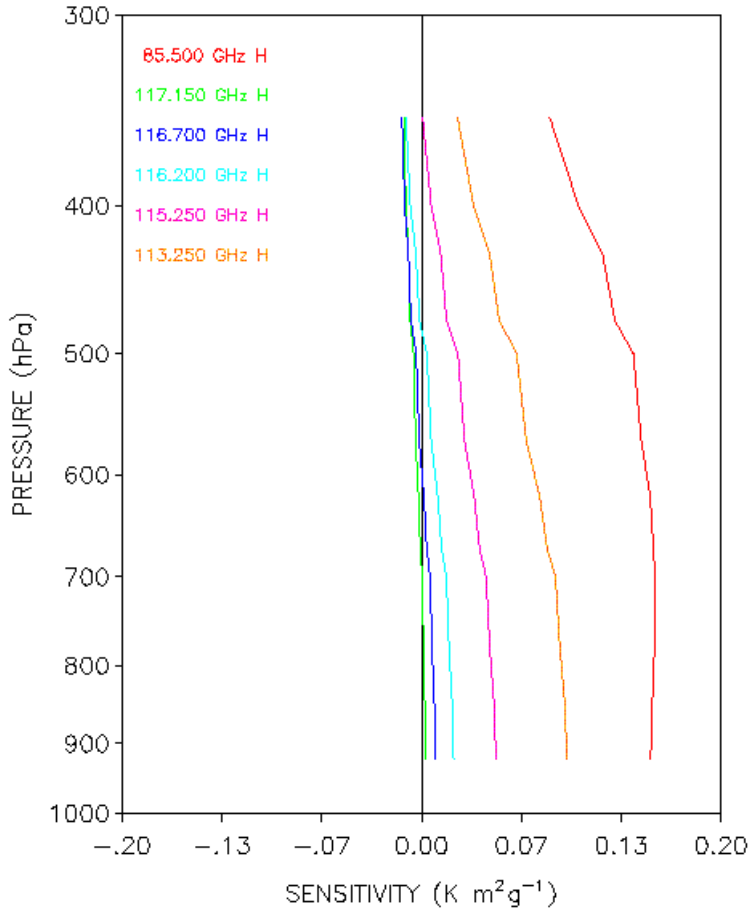

Figure 2-2: The sensitivity of brightness temperatures, at the labeled frequencies, to a perturbation in cloud liquid water. The temperature and moisture profiles are for global mean. The surface emissivity is for ocean and the base-state atmosphere is clear, so the conditions are relatively favorable for cloud sensitivity.

2.5 Requirements for cross sensor data

No cross-sensor data are required for CLW EDR retrieval. When VIIRS data are available to identify cloud-free scenes, the performance for those scenes is enhanced from what would be obtained in a CMIS-only retrieval. Performance may also be enhanced by using VIIRS to evaluate inhomogeneity of the cloud field within a CMIS field of view.

2.6 Requirements for External Data

The only external data required to achieve threshold performance for the CLW EDR is surface pressure, derived from combination of NWP model forecast data, and terrain heights from a high-spatial-resolution global topography database.

2.7 Summary of Derived Requirements on the EDR Algorithm

For CLW retrieval in non-precipitating conditions, the algorithm requires CLW data from the Core Module with the characteristics specified in Table 2-2.

Table 2-2: CLW requirements placed on the Core Module by the CLW Algorithm.

Parameter	Thresholds
a. Horizontal Spatial Resolution	24 km
b. Horizontal Reporting Interval	20 km
c. Vertical Cell Size	N/A (Total Column)
d. Vertical Reporting Interval	N/A (Total Column)
e. Horizontal Coverage	Global
f. Vertical Coverage	N/A (Total Column)
g. Measurement Range	0 - 5 kg/m^2
h. Measurement Uncertainty	
1. Over ocean	0.03 kg/m^2
2. Over land	0.19 kg/m^2
i. Mapping Uncertainty	7 km
j. Swath Width	1700 km

3 Algorithm Description

3.1 Historical and Background Perspective of Proposed Algorithm

A variety of physical and statistical algorithms have been used for CLW retrieval from passive microwave data over oceans. Regression algorithms trained from model data (Chang and Wilheit, 1979) and from empirical data (Alishouse et al., 1990) have been widely used. Phalippou (1996) used a variational phyisical method, which is similar to the CMIS core module, in the context of numerical weather prediction. For algorithms designed to address a range of clouds from non-precipitating through precipitating, it has been found beneficial to segment the algorithm so that it can better respond to the different radiative responses that dominate for different amounts of cloud and precipitation (Liu and Curry, 1993; Weng and Grody, 1994).

For CLW retrievals over land, physical methods exploiting thermal contrast (Jones and Vonder Haar, 1990) and attenuation of surface polarization signal (Greenwald, et al., 1997) have been developed and evaluated for the Special Sensor Micowave/Imager (Greenwald, et al., 1999). These algorithms rely on ancillary surface, radiosonde, and infrared satellite observations to help distinguish cloud signals from variability in other atmosphere and surface parameters.

3.2 Theoretical and Mathematical Description of Algorithm

3.2.1 Non-precipitating clouds

The primary retrieval function for non-precipitating clouds is performed by the Core Physical Inversion Module. The algorithm exploits both the thermal contrast and depolarization phenomena. It incorporates data from multiple channels simultaneously, relying on channels in proportion to their sensitivity to CLW in each given scene. The module retrieves cloud top pressure and cloud thickness simultaneously with the total cloud liquid water, minimizing the extent to which errors in cloud altitude project into errors in CLW. The core module makes use of a dynamic surface emissivity database, which substantially improves performance over land surfaces. The benefits of such local, timely emissivity data were demonstrated by Jones and Vonder Haar (1990) in their CLW retrievals over land. Details of the core module are in ATBD Vol. 2. The CLW algorithm does no further retrieval processing in non-precipitating conditions.

3.2.2 Precipitating clouds

The algorithm for precipitating clouds is designed to retrieve the total liquid water path (LWP), including suspended and precipitating liquid, in view of the discussion in Sec. 2.3. The retrieval is performed within the Precipitation Module. This integrated approach ensures consistency between the precipitation and CLW EDR products.

Over ocean, the liquid water path is diagnosed as part of the precipitation retrieval. The ocean precipitation algorithm relies on inverting a spectral normalized polarization difference, P, which can be represented as

$$P = \frac{T_{B,V} - T_{B,H}}{T_{B,V0} - T_{B,H0}} = \exp\left[-\frac{\alpha R^{\beta} H + \kappa_{ext,L} CLW}{\cos\theta} \right],$$

where T_B is brightness temperature, subscripts V and H refer to polarization, the subscript 0 refers to clear-sky values, R is the rain rate, H is the depth of the rain layer, θ is the zenith angle, and $\kappa_{ext,L}$ is the extinction coefficient for cloud liquid. The precipitation algorithm assumes a Marshall-Palmer drop size distribution and infers H from the freezing level, such that P can be represented in terms of the rain water path (RWP) rather than R:

$$P = \exp\left[-\frac{\kappa_{ext,R} RWP + \kappa_{ext,L} CLW}{\cos\theta} \right],$$

where $\kappa_{ext,R}$ is the extinction coefficient for rain water. The LWP is computed as the sum of RWP and CLW. The precipitation algorithm must make an assumption about how much of the LWP resides in CLW so that it can infer R. The LWP retrieval is less sensitive to that assumption than the R retrieval is, since the allocation between RWP and CLW affects the LWP retrieval only to the extent that $\kappa_{ext,R}$ and $\kappa_{ext,L}$ differ. The LWP retrieval is thus not only consistent with the R retrieval, but is also a little less subject to error. A major additional benefit of treating the LWP within the ocean precipitation algorithm is that the LWP retrieval benefits from the two-dimensional processing method that allows the low-frequency (10 GHz) channels to contribute to the high-spatial-resolution retrieval.

Over land, a neural network method is used. The rationale for the approach, the network design, and the data used to train and test the network are described in ATBD Vol. 5: Precipitation.

3.2.3 Algorithm processing outline

A mechanism is needed to ensure a smooth transition between the products of the algorithms for non-precipitating and precipitating clouds. The core module provides quality-control parameter, which provides an indication whether precipitation affected the CLW retrieval. The core module product may be reliable for marginal precipitation because the module tracks and responds to quality indicators to exclude the highest frequency channels that are most sensitive to precipitation effects. When a precipitation influence is detected, the core module product is considered unreliable because precipitation is not included in the core module radiative transfer model. In such cases, the product from the precipitating cloud module is used for the CLW product.

For clouds that are on the threshold of precipitating, the core module and the algorithm for precipitating clouds may produce different results. As long as there is a strong correlation between the results of the two algorithms in the transition range, the CLW product will transition smoothly between the non-precipitating and precipitating regimes. If, in the course of validation, it is found that the correlation is not sufficiently strong, a smoother can be applied. An option for such a smoother is a weighted average. A candidate weighting scheme is a hyperbolic tangent weight

$$w_{precip} = \frac{1}{2}\left[\tanh\left(S_{trans}\left(LWP_{precip} - LWP_{trans}\right)\right)+1\right],$$

where LWP_{precip} is the product of the precipitating cloud algorithm, w_{precip} is the weight assigned to it, LWP_{trans} is the defined transition point, and S_{trans} is the defined scale factor for the transition. The weighting may also be modulated by the expected error of each product, derived from validation exercises.

3.3 Algorithm Processing Flow

3.3.1 Processing Flow for the CLW algorithm

The processing flow for the CLW algorithm is illustrated in Figure 3-1.

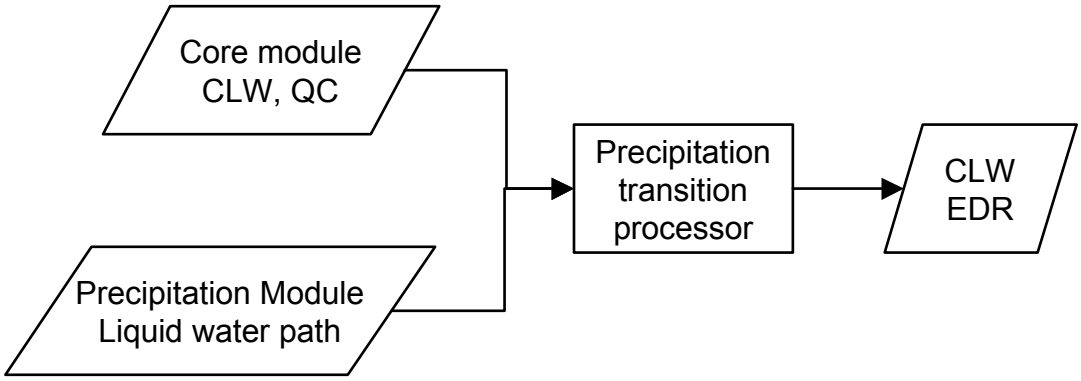

Figure 3-1: Processing flow diagram for the CLW algorithm

3.3.2 Algorithm inputs

Table 3-1: CLW algorithm inputs

Data	Type	Source	Usage
Latitude/longitude at surface	"	SDR	EDR reporting
Time/date	"	SDR	EDR reporting
Cloud liquid water	"	Core module	EDR product generation
Quality control parameters	"	Core module	EDR product generation and reporting
Cloud top pressure	"	Core module	EDR reporting
Cloud top thickness	"	Core module	EDR reporting
Liquid water path	"	Precipitation module	EDR product generation

3.3.3 Algorithm outputs

Table 3-2: CLW algorithm outputs

Output parameter
Cloud liquid water
Cloud top pressure
Cloud top thickness
Quality flag
Latitude/longitude at surface
Time/date

3.3.4 Integration of CLW algorithm in the CMIS EDR algorithm set

The algorithm for precipitating clouds is essentially the same as the algorithms used to retrieve cloud ice water path in precipitating conditions and precipitation rate over land, thus providing consistency between these EDR algorithm products.

The CLW algorithm is executed after the core module is executed on 20-km Composite Field of View (CFOV) data.

4 Algorithm Performance

4.1 Description of Test Data and Test Methods

The test data for evaluating the CLW for non-precipitating clouds consist of the data applied to the core module, described in ATBD Vol. 2. The test data for precipitating clouds are described in ATBD Vol. 5: Precipitation.

4.2 Sensitivity Studies

4.2.1 Two-path scene contrast

Cloud liquid water is highly inhomogeneous in the atmosphere, with substantial variations over short spatial scales being common even for stratified cloud types. With such inhomogeneities, there may be differences in cloud between the direct and indirect paths over which radiation reaches the satellite. The direct path follows the satellite view vector from the surface to the satellite. The indirect path refers to downwelling radiation that is reflected by the surface before being transmitted to the satellite. The greatest differences would occur when the surface reflection is specular and highly reflective and the scene has a gradient in CLW oriented along the cross-scan direction. Ocean scenes are relatively stressing, because they have relatively high surface reflectance. Differences are also sensitive to cloud height, since the direct and indirect paths traverse the same cloud field when the cloud is adjacent to the surface.

One means to address this phenomenon is to retrieve cloud liquid separately for the direct and indirect paths. We performed sensitivity experiments with such a version of the core module, where the constraint on the correlation between two CLW values was varied. These sensitivity experiments were performed for ocean scenes under the assumption of perfect specularity. We

considered path CLW differences of 0.1 kg/m^2, which we estimate to be relatively large for non-precipitating clouds at 20-km CFOV size. The radiometric noise imposed on the simulated data was for 15-km CFOV size. The results are summarized in Table 4-1. In the table, the variable r is the imposed correlation between CLW in the two paths. For $r = 1$, the retrieval is effectively assuming cloud is the same in both paths. For the clear case (0 CLW in both paths), the errors are very small regardless of the treatment. With the direct path clear and the indirect path cloudy, the errors are still small, but are substantially larger than for the clear case and there is a modest benefit of making two-path retrievals ($r \neq 1$). When the direct-path CLW is relatively large, the direct-path cloud obscures the indirect-path signal and the standard retrieval approach ($r = 1$) is the most skillful of the methods tested. Overall, the results indicated that the standard approach was the best option, but that differences in cloud between the two paths can induce significant errors.

Table 4-1: CLW retrieval performance with various treatments of path contrasts. All parameters are in units of kg/m^2.

		Direct-path retrieval rms error			Indirect-path retrieval rms error		
Direct true CLW	Indirect true CLW	$r = 0$	$r = 0.5$	$r = 1$	$r = 0$	$r = 0.5$	$r = 1$
0.0	0.0	0.01	0.01	0.01	0.02	0.02	0.01
0.0	0.1	0.04	0.04	0.06	0.04	0.04	0.05
0.3	0.2	0.12	0.07	0.05	0.11	0.07	0.05
0.3	0.3	0.08	0.04	0.02	0.08	0.04	0.02

4.2.2 Partial cloud cover

The radiative transfer in the core module has the cloud fraction set to unity by default, which means that the retrievals are made under the assumption of complete cloud cover. In previous work with other microwave instruments, we had found retrieval of cloud cover to be infeasible because the algorithm does not have sufficient radiometric information to distinguish cloud cover variations from cloud liquid water variations.

The effect of partial cloud cover on CMIS performance was evaluated by considering cases with 50% cloud cover. The simulations included a uniform random distribution of CLW from 0 to 0.5 kg/m^2 within the cloudy portion of the scene. Verification was done against the average CLW over the entire scene. For comparison, a set of retrievals were performed on test cases with the

same scene-average CLW, but with complete cloud cover. Over land scenes, the impact was about 5% proportional increase in error. Over the surface where the radiometric data are most sensitive to cloud effects, oceans, the rms retrieval errors were 0.015 kg/m^2 (unbinned) for uniform cloud cover and 0.039 kg/m^2 for 50% cloud cover. The binned performance plots (Figure 4-1) indicate minimal impact for low values of the true CLW and increasing impact for higher CLW values. Most of the added error is attributable to a negative bias (Figure 4-2).

The results follow from the physics of cloud radiative transfer. When the CLW is low, the cloud is optically thin in the microwave and a change in CLW in the cloudy portion of the field of view (FOV) is linearly related to the brightness temperatures. A change in cloud fraction has the same linear relationship, so the retrieval responds the same whether the CLW is limited to a portion of the FOV of spread over the entire FOV. When the CLW is high, the brightness temperatures are no longer linearly related to the CLW and the brightness temperatures are less sensitive to changes in CLW. This non-linearity is the familiar phenomenon of saturating instrument response (Weng and Grody, 1994). In this case, a given set of brightness temperatures could correspond to a certain CLW spread across the FOV or could correspond equally to a higher CLW limited to a portion of the FOV, and a negative bias is introduced in the retrievals.

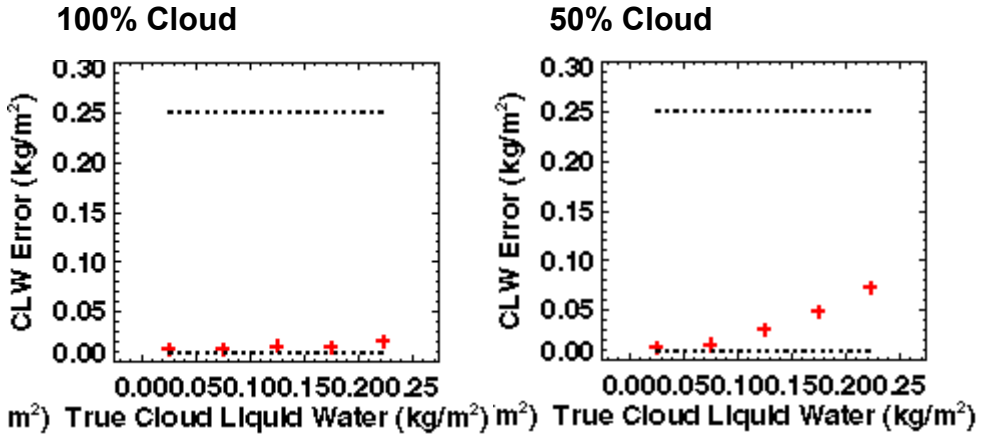

Figure 4-1: CLW rms retrieval error for complete (left) and 50% (right) cloud cover over ocean scenes. Retrievals were for a 20-km CFOV.

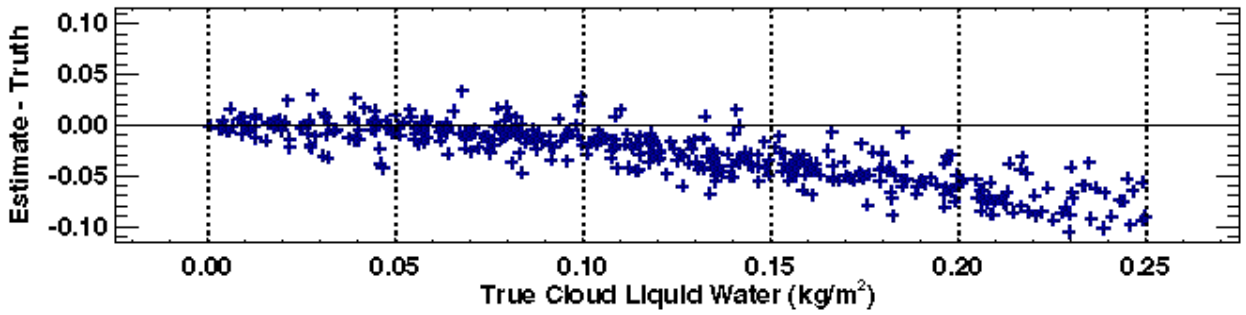

Figure 4-2: Scatterplot of CLW retrieval error versus true value for cases with 50% cloud cover over ocean.

One option to address cloud cover effects is to alter the channel selection. The absorption coefficient for cloud liquid is a monotonically increasing function of frequency throughout the microwave spectrum. An implication is that higher frequency channels are better able to detect and retrieve small amounts of CLW but, at the same time, they are more susceptible to the saturation phenomenon that induces retrieval errors in partial cloud cover (Figure 4-3). This tradeoff was explored by performing retrievals for 100% and 50% cloud cover over ocean, as before, but while excluding all channels with frequencies above 60 GHz. Exclusion of the higher frequencies improves performance somewhat for conditions with 50% cloud cover, but degrades performance substantially for 100% cloud cover (Table 4-2). As expected, the performance is less sensitive to cloud fraction when the higher frequencies are excluded. Whether it is beneficial overall to exclude the higher frequencies depends on the frequency distribution of cloud fraction over the global oceans. Here, we are referring specifically to cloud fraction when measured on the scale of 20-km cells. A further evaluation of this tradeoff is deferred to test and validation efforts in later phases of CMIS development, and inclusion of the higher frequency channels remains the baseline.

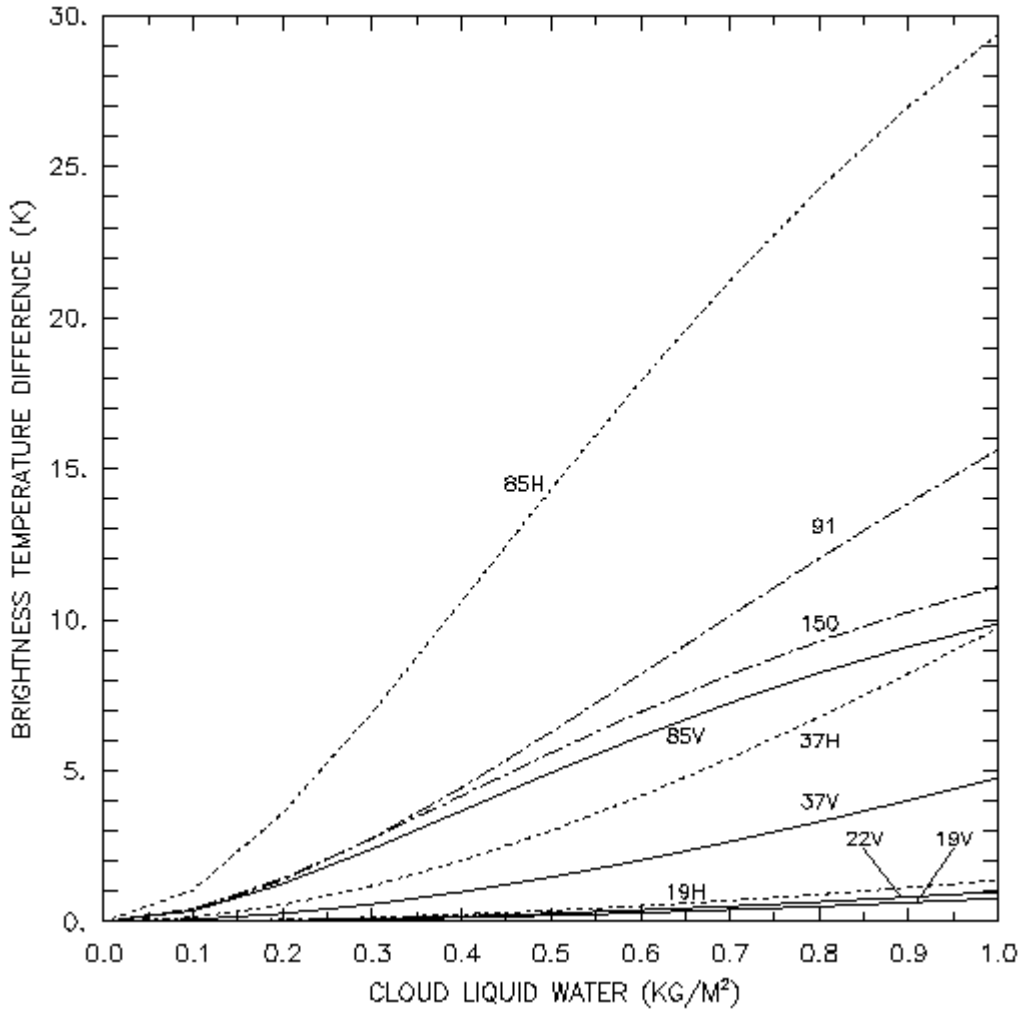

Figure 4-3: The impact of fractional cloud cover on window channel brightness temperatures, for simulations of conically-viewing SSM/I channels at 85, 37, 19, and 22 GHz and nadir viewing SSM/T-2 channels at 91 and 150 GHz. The V and H labels indicate the polarization state. The curves are the difference between brightness temperatures obtained with 50% cloud cover and CLW=x, and 100% cloud cover and CLW=x/2, where x is the horizontal axis of the plot. The calculations are for a midlatitude profile and a cloud top of 600 mb. Note the effect is largest for 85 GHz horizontal polarization.

Table 4-2: CLW performance tradeoff for channel selection and cloud fraction. Retrieval errors are in kg/m^2.

	100% cloud cover	50% cloud cover
Full channel set	0.015	0.039
Exclude channels > 60 GHz	0.026	0.032

The CMIS algorithm is capable of incorporating external cloud fraction data into the core module retrieval. In particular, a pixel-scale cloud mask from VIIRS may be weighted against the CMIS CFOV spatial response function to provide a cloud fraction to the core module. With reliable cloud fraction data, the CMIS performance is expected to depend little on cloud fraction. Where the mask is unavailable or is flagged as unreliable, the core module can revert to the assumption of complete cloud cover.

4.3 Performance in non-precipitating conditions

CLW retrieval performance is highly sensitive to surface type and, in particular, to the surface emissivity at 18/23 GHz and its uncertainty. Further discussion of surface types, their relationship to emissivity, and their frequency of occurrence are in ATBD Vol. 3: Water Vapor EDRs. Binned performance for several surface types is illustrated in Figure 4-4.

The core module algorithm has an option to use a dynamic emissivity database, developed from local emissivity statistics, to provide the constraint on the emissivity spectrum, as an alternative to using climatological databases. In regions were emissivities are stable (e.g., no recent precipitation), we estimate the 18/23 GHz emissivity uncertainty from the dynamic database will be approximately 0.005. The impact on performance is demonstrated in the lower two frames of Figure 4-4 for mixed forest. For high-emissivity surfaces, such as forests, there is substantial retrieval skill when the local, dynamic emissivity database is used, whereas there is virtually no skill without the local emissivity data.

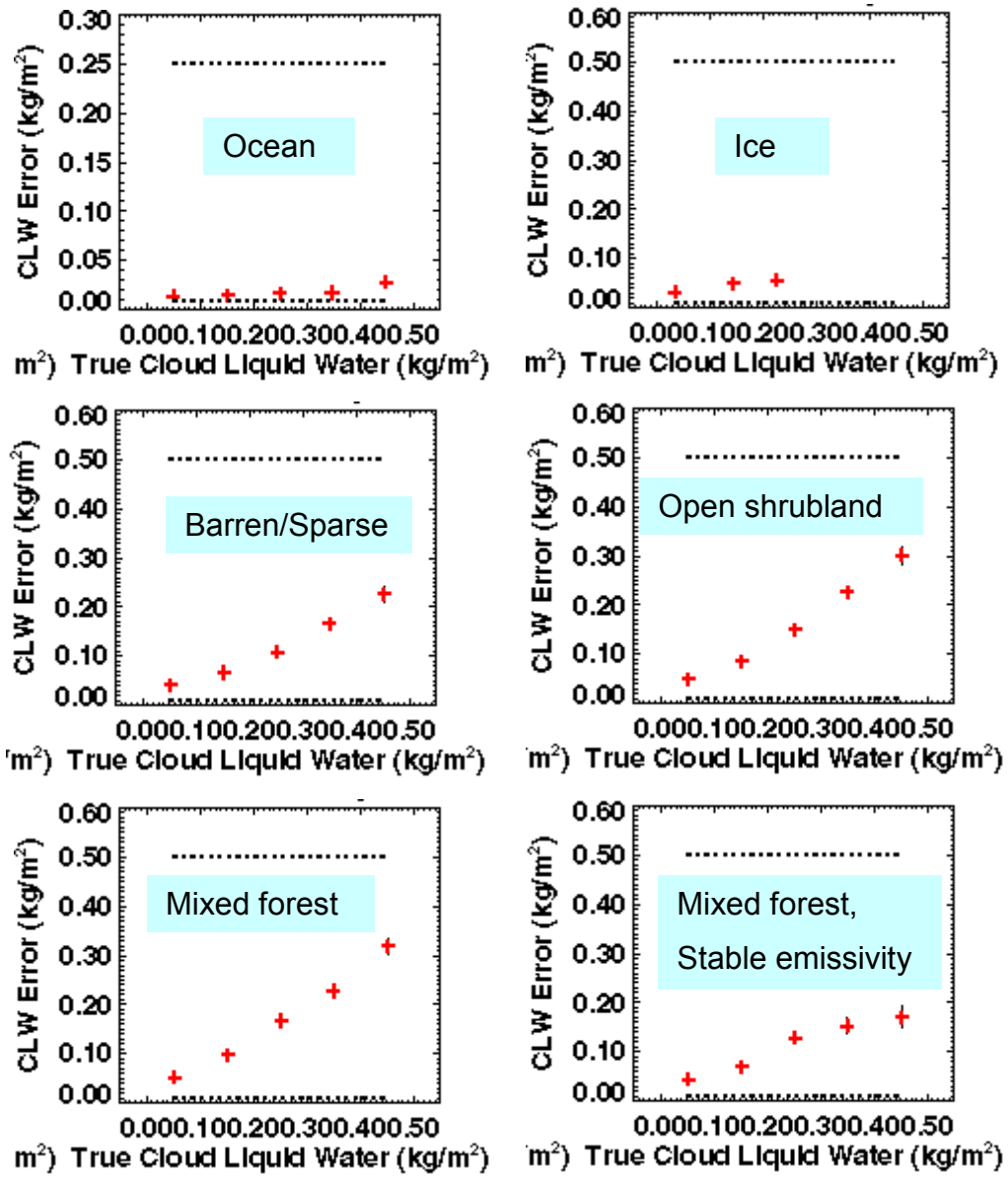

Figure 4-4: CLW measurement uncertainty (rms error) for various surface types. The thresholds and objectives are marked as dotted lines. Note the vertical scale is different in the "ocean" frame.

4.4 Performance in precipitating conditions

Binned performance for precipitating clouds is in Figure 4-5 for ocean surfaces. A relatively high degree of skill is maintained across the measurement range due to the range of frequencies that are used, including the 10 GHz channel for sensitivity with the larger values of CLW. Binned performance for precipitating clouds over land are in Figure 4-6. Over land, where use

of the 10 GHz is not practical, the measurement range is limited by the lack of sensitivity to large CLW. The higher values of CLW correspond also to higher values of ice water path, where the ice overlays and coexists with the liquid in the scenes. While the statistical land algorithm can exploit correlations between ice and liquid, the relationship is not reliable enough to prevent an upturn in the retrieval error at high CLW. (See also EN #46 response.)

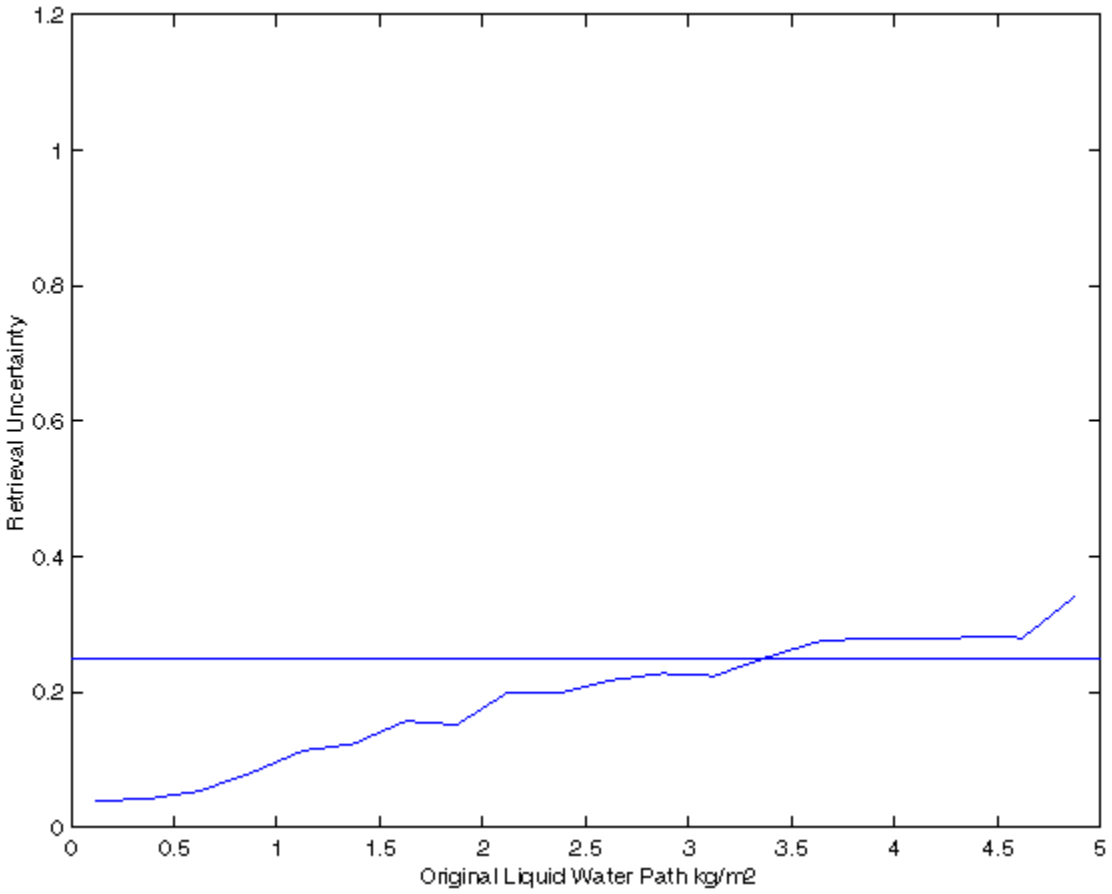

Figure 4-5: CLW measurement uncertainty for precipitating clouds over ocean.

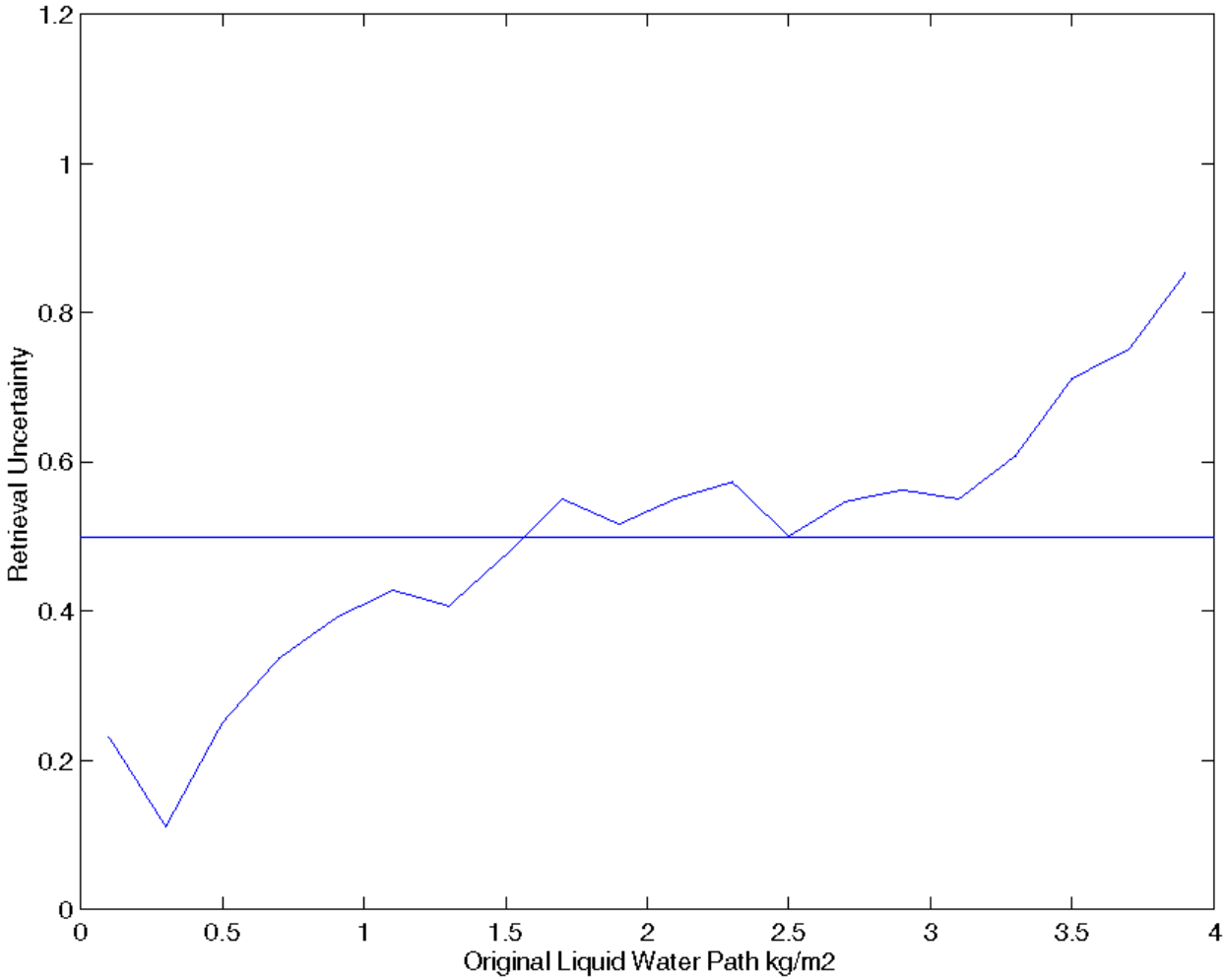

Figure 4-6: CLW measurement uncertainty for precipitating clouds over land.

4.5 Performance summary

The nominal performance for the CLW EDR is summarized in Table 4-3. The error budget is in Table 4-4, and covers nominal conditions and degraded measurement conditions (heavier precipitation) summarized in Table 4-6. The error estimates were made from retrievals performed directly at 20-km CFOV size, under the assumption that the cascade (see ATBD Vol. 1: Integration) would have negligible effect on CLW performance, given that cloud varies on short spatial scales. Performance is computed in bins that span the measurement range and the quoted performance refers to the worst-case bin unless otherwise specified. For non-precipitating clouds, the measurement range is taken to be 0 to 0.5 kg/m^2.

The requirement to use the worst-case bin for CMIS performance has a major impact on the magnitude of the quoted errors. As an example, the default core module retrieval simulation for non-precipitating clouds over ocean produced a worst-case bin error of 0.028 kg/m^2, which grows to 0.08 kg/m^2 with budgeting of additional error terms. Alternatively, we can estimate global average performance by taking the binned performance and weighting according to an exponential frequency distribution of CLW (Wentz, 1997) corresponding to a global-mean CLW of 0.08 kg/m^2 (Greenwald, et al., 1993). The result is an error of 0.014 kg/m^2, which grows to 0.034 kg/m^2 with error budgeting for global average conditions. Similarly, the net error for non-precipitating land cases is about 0.07 kg/m^2 for the global average.

Table 4-3: Nominal performance for the CLW EDR.

Parameter	Thresholds	Performance
a. Horizontal Cell Size	20 km	20 km
b. Horizontal Reporting Interval	20 km	20 km
c. Vertical Cell Size	N/A (Total Column)	N/A (Total Column)
d. Vertical Reporting Interval	N/A (Total Column)	N/A (Total Column)
e. Horizontal Coverage	Global	Global
f. Vertical Coverage	N/A (Total Column)	N/A (Total Column)
g. Measurement Range	0 - 5 kg/m^2	0 - 5 kg/m^2
h. Measurement Uncertainty		
1a. Over ocean, non-precipitating	0.25 kg/m²	0.08 kg/m²
1b. Over ocean, precipitating	0.25 kg/m²	0.23 kg/m²
2a. Over land, non-precipitating	0.5 kg/m²	0.21 kg/m²
2b. Over land, precipitating	0.5 kg/m²	0.45 kg/m²
i. Mapping Uncertainty	7 km	3 km
j. Swath Width	1700 km (TBR)	1700 km

The row in Table 4-4 denoted "Default core module retrieval error" refers to the error sources incorporated into the default retrieval simulations, including smoothing (null-space) and radiometric noise. Following that row are several rows (up to "Subtotal") for which the errors are additive. The numbers cited are the added retrieval errors that were found as each error source was individually simulated.

For precipitating clouds, the performance was addressed by considering a range of surface types simultaneously. The values in the columns for non-precipitating clouds in Table 4-4 were derived by considering the range of surface types summarized in Table 4-5. The net nominal performance combines the performance for conditions where the dynamic surface emissivity

database can be applied ($\sigma(\varepsilon_s) \leq 0.005$) with those where the algorithm relies on global emissivity constraints with preclassification. The "proportion" column indicates the weighting between the two conditions. An exception is the ocean surface, for which the emissivity database is not needed. The net nominal performances for land are combined by the frequency of occurrence of each type.

Where an error budget entry is zero, that indicates that the error term is negligible in relation to the other terms, not that the error term is identically zero.

The error budget includes two terms for spectroscopic errors. One refers to the biases between the brightness temperatures CMIS reports and brightness temperatures simulated by applying the core module radiative transfer to data representing the true environmental conditions. It is a residual in the sense that these biases are largely corrected before the water vapor retrievals are performed, using correction factors derived from calibration/validation with ground truth data (Wentz, 1997). Some differences between the CMIS measurements and the model are not sufficiently systematic to be corrected with ground truth data, and the budget includes a separate term for these errors. The error increments for ocean and land are 5% and 0.5%, respectively, of the nominal error.

The budget includes a term for differences between CLW in the direct and indirect paths. Considering the varying degree of ocean surface specularity and of cloud path differences on the 20-km scale, we estimate an error increment of 60% for non-precipitating clouds. The effect of partial cloud cover, averaged over the oceans, is estimated as an error increment of 100% for non-precipitating clouds. Increments of 40% and 70%, respectively, are used for these error sources for precipitating clouds, accounting for the tendency of precipitating clouds to have larger spatial scales than non-precipitating clouds.

Spatial coregistration errors involve two factors. One is the divergence of two beams that are coregistered at the surface but have different Earth incidence (zenith) angles and, hence, slightly different paths through the atmosphere. An analysis of this factor found no significant effect on CLW retrieval. The other factor is the uncertainty in the position of each channel's beam in relation to the positions of other channels. This factor was evaluated by considering several types of scene spatial structure that could cause brightness temperatures in a misregistered channel to be different from a correctly registered channel. Effects of cloud, surface emissivity,

and surface temperature structure were considered and the impact on retrieval performance was computed. Details of the analyses are in Appendix A of ATBD Vol. 1, Part 1: Integration. For the CLW EDR, coregistration errors within the requirements flowed to the sensor could cause retrieval error to increase by 5% of the retrieval error obtained without coregistration error. The factor was negligible over land.

The channels on CMIS are not all boresighted, so there are time offsets on the order of a few seconds between the views of the various channels. An analysis indicated that the time offsets have no significant impact on retrievals.

Uncertainty in the surface pressure, provided as external data to the core module, was found experimentally to have a very small impact on CLW performance (about 1% proportional increase in error).

Errors are introduced by the difference in spatial weighting between the horizontal cells used for validation (uniform averaging over a square) and the composite antenna pattern represented by the CFOV. Analysis of this effect is discussed in Appendix TBD of ATBD Vol. 1, Part2: Footprint Matching and Interpolation. These errors are listed as "cell mismatch error" in the budget.

Table 4-4: Error (kg/m^2) budget for CLW EDR

	Ocean		Land	
Term	Non-precipitating	Precipitating	Non-precipitating	Precipitating
Default core module retrieval error	0.028	0.1 or 9%	0.192	0.42 or 32%
Residual calibration/model bias	0.002	0.005 or 0.5%	0.001	0.002 or 2%
Residual unsystematic spectroscopic error	0.002	0.005 or 0.5%	0.001	0.002 or 2%
Direct/indirect-path differences	0.017	0.04 or 3.6%	0.000	0.00 or 0%
Partial cloud cover	0.028	0.07 or 6.3%	0.010	0.025 or 2%
Channel spatial coregistration error	0.002	0.005 or 0.5%	0.000	0.00 or 0%
Channel temporal	0.000	0.000 or 0%	0.000	0.00 or 0%

offset				
Surface pressure error	0.000	0.001 or 0%	0.002	0.00 or 0%
Subtotal	0.079	0.226 or 20.4%	0.206	0.45 or 38%
Cell mismatch	0.016	0.016 or 1%	0.016	0.02 or 1%
Net	0. 081	0.227 or 21%	0.207	0.45 or 38%

Table 4-5: CLW EDR performance (rms error in kg/m^2) for non-precipitating clouds for various surface conditions (19 GHz H-polarization) and other measurement conditions.

$\sigma(\varepsilon_s) \leq 0.005$	Proportion	Ocean	Land ≤ 0.80	Land 0.80 - 0.86	Land 0.86 - 0.90	Land 0.90 - 0.98	Land Net
N	50%	0.028	0.057	0.226	0.300	0.318	
Y	50%		0.015	0.066	0.124	0.171	
Net Nominal:		0.028	0.036	0.146	0.212	0.245	0.192
% Coverage:		N/A	15.2	16.9	13.6	54.3	

4.6 Summary of performance under degraded measurement conditions

Performance under degraded measuring conditions is summarized in Table 2-1. The degraded sensitivity to cloud liquid as precipitation intensifies leads to increasing absolute measurement errors for larger CLW. Performance of sea ice is comparable to performance over land.

Table 4-6: Summary of CLW performance under degraded measurement conditions.

Condition	Indicator	Measurement uncertainty
Moderate precipitation over ocean	CLW ≥ 1 kg/m^2	21%
Moderate precipitation over land	CLW ≥ 1.2 kg/m^2	38%
Sea ice, non-precipitating	Detectable ice within 100 km	0.2 kg/m^2
Sea ice, precipitating	Detectable ice within 100 km	0.45 kg/m^2 or 38%

Excluded from performance are conditions outside a measurement range of 0-3 kg/m^2 over land or ice surfaces. (See also EN # 46 response.)

4.7 Special considerations for Cal/Val

4.7.1 Measurement hardware

4.7.2 Field measurements or sensors

4.7.3 Sources of truth data

5 Practical Considerations

5.1 Numerical Computation Considerations

5.2 Programming/Procedure Considerations

5.3 Computer hardware or software requirements

5.4 Quality Control and Diagnostics

5.5 Exception and Error Handling

5.6 Special database considerations

5.7 Special operator training requirements

5.8 Archival requirement

REFERENCES

Alishouse, J. C., J. B. Snider, E. R. Westwater, C. T. Swift, C. S. Ruf, S. A. Snyder, J. Vongsathorn, and R. R. Ferraro, 1990: Determination of cloud liquid water content using the SSM/I. *IEEE Trans. Geosci. Remote Sensing*, **28**, 817-821.

Bohren, C. F., and D. R. Huffman, 1983: *Absorption and Scattering of Light by Small Particles*. Wiley, New York.

Chang, A. T., and T. T. Wilheit, Remote sensing of atmospheric water vapor, liquid water, and wind speed at the ocean surface by passive microwave techniques from the Nimbus 5 satellite. *Radio Sci*., **14**, 793-802.

Gasiewski, A. J., 1992: Numerical sensitivity analysis of passive EHF and SMMW channels to tropospheric water vapor, clouds, and precipitation. *IEEE Trans. Geosci. Remote Sensing*, **30**, 859-870. Errata: 1993, **31**, 306.

Greenwald, T. J., G. L. Stephens, T. H. Vonder Haar, and D. L. Jackson, 1993: A physical retrieval of cloud liquid water over the global oceans using Special Sensor Microwave/Imager (SSM/I) observations. *J. Geophys. Res*., **98**, 1847-1848.

Greenwald, T. J., C. L. Combs, A. S. Jones, D. L. Randel, and T. H. Vonder Haar, 1997: Further developments in estimating cloud liquid water over land using microwave and infrared satellite measurements. *J. Appl. Meteor*.,**36**, 389-405.

Greenwald, T. J., C. L. Combs, A. S. Jones, D. L. Randel, and T. H. Vonder Haar, 1999: Error estimates of spaceborne passive microwave retrievals of cloud liquid water over land. *IEEE Trans. Geosci. Remote Sensing*, **37**, 796-804.

Jones, A. S., and T. H. Vonder Haar, 1990: Passive microwave remote sensing of cloud liquid water over land regions. *J. Geophys. Res*., **95**, 1667-1668.

Lipton, A. E., M. K. Griffin, and A. G. Ling, 1999: Microwave transfer model differences in remote sensing of cloud liquid water at low temperatures. . *IEEE Trans. Geosci. Remote Sensing*, **37**, 620-623.

Liu, G., and J. A. Curry, 1993: Determination of characteristic features of cloud liquid water from satellite microwave measurements. *J. Geophys. Res*., **98**, 5069-5092.

Phalippou, L., 1996: Variational retrieval of humidity profile, wind speed and cloud liquid-water path with the SSM/I: Potential for numerical weather prediction. *Quart. J. Roy. Meteor. Soc*., **122**, 327-355.

Weng, F., and N. C. Grody, 1994: Retrieval of cloud liquid water using the special sensor microwave imager (SSM/I). *J. Geophys. Res*., **99**, 2553-2555.

Wentz, F. J., A well calibrated ocean algorithm for SSM/I, *JGR*, **Vol 102**, pp 8703-8718, 1997.

LIST OF ACRONYMS

AER	Atmospheric and Environment Research
ATBD	Algorithm Theoretical Basis Document
CFOV	Composite Field of View
CLW	Cloud Liquid Water
CMIS	Conical-Scanning Microwave Imager/Sounder
EDR	Environmental Data Record
FOV	Field Of View
IPO	Integrated Program Office
LWP	Liquid Water Path
NPOESS	National Polar-orbiting Operational Environmental satellite System
QC	Quality Control
SDR	Sensor Data Record
SRD	Sensor Requirement Document
SSM/I	Special Sensor Mirowave/Imager
SSM/T-2	Special Sensor Mirowave/Temperature-2
TBD	To Be Determined (by contractor)
TDR	Temperature Data Record
VIIRS	Visible/Infrared Imager/Radiometer Suite